# Theoretical calculation of single ionization in collisions between protons and low-$Z$ molecules at intermediate and high energies

M. E. Galassi and R. D. Rivarola
*Instituto de Física de Rosario (CONICET-UNR), Avenida Pellegrini 250, 2000 Rosario, Argentina*

M. Beuve
*Centre Interdisciplinaire de Recherches Ion-Laser, Boîte Postale 5133, 14070 Caen, France*

G. H. Olivera
*Department of Medical Physics, Medical School, University of Wisconsin-Madison, 1530 Medical Sciences Center, 1300 University Avenue, Madison, Wisconsin 53706-1532*

P. D. Fainstein*
*Centro Atómico Bariloche, Comisión Nacional de Energía Atómica, Avenida E. Bustillo 9500, 8400 Bariloche, Argentina*
(Received 16 February 2000; published 5 July 2000)

Single ionization total cross sections for proton impact on $N_2$, CO, $CH_4$, and $CO_2$ are calculated by applying the continuum-distorted-wave-eikonal-initial-state model. Two different approximations have been considered for molecular targets: Bragg's additivity rule and a molecular representation of the bound state target wave function. In the latter, the cross section is approximated by a linear combination of atomic cross sections where the coefficients are determined from a population analysis and the binding energies have been extracted from experimental spectra. The results from both models are compared with experimental data.

PACS number(s): 34.50.Fa, 34.50.Gb

## I. INTRODUCTION

Knowledge of differential and total ionization cross sections is of great interest in many areas such as atmospheric, plasma, and biological physics. In particular, an important application of these results is in the area of radiotherapy. When a human tissue is exposed to the action of ionizing radiation several changes can take place at random in the cellular genetic code (mutations). These changes have their origin, in most cases, in the ionization of the DNA structure either from the direct action of the radiation or by the formation of free radicals in its vicinity. The nature and probability of the biological damage due to the DNA damage depends on the density of the energy deposited along the trajectory of the beam that intersects the DNA and also on the complex interrelation between damage and enzymatic repair of the cell. A magnitude that is used to quantify the interaction of the radiation with the matter is the absorbed dose, which is defined as the expectation value of the energy imparted to matter per unit mass at a point. To calculate the absorbed dose for an irradiated material it is required to know the spatial distribution of the deposited energy. The energy densities should be calculated as functions of the position and of the time, employing the differential and total cross sections of excitation and ionization that describe these processes in the atoms and molecules of the biological target. Since live matter is constituted not only of complex molecular chains, but also of such simple molecules as $N_2$, $O_2$, $CH_4$, CO, $H_2O$, and $CO_2$, cross sections for ionization of these molecules by the impact of heavy ions are also of great interest.

In previous works we have studied the energy loss of protons in $O_2$ and $H_2O$ molecular targets [1]. It was observed that the results improved, especially at intermediate energies, when the molecular character of the target was considered and high-order theoretical models were used to calculate the single ionization cross section. These results gave a clear indication of the limited validity of Bragg's additivity rule and of first-order theoretical models like the first Born approximation.

In the present work we calculate doubly differential (DDCS) and total cross sections (TCS) for single ionization of several molecular targets ($N_2$, CO, $CH_4$, $CO_2$) by proton impact. In each case we perform a population analysis that allows us to develop the molecular wave function in a linear combination of atomic orbitals. For each orbital the transition amplitude is calculated using the continuum-distorted-wave-eikonal-initial-state (CDW-EIS) model [2,3]. The results are compared with the available experimental data [4–6].

## II. THEORY

### A. Theoretical model

The basic difficulty in modeling the single ionization process in ion-atom or ion-molecule collisions at intermediate to high energies arises from the long range of the Coulomb interaction between all the charged particles. In the initial channel, the projectile field will distort the initial bound state, while in the final channel, the emitted electron will travel in the combined fields of the residual target and projectile. Furthermore, there is an additional difficulty introduced by the fact that the target is a multielectronic atom or molecule. A convenient way to treat this problem in perturbation theory is through the distorted-wave formalism and by

*Electronic address: pablof@cab.cnea.gov.ar

 

TABLE I. Population and binding energies of the $N_2$ molecular orbitals.

| Molecular orbital | Population | Binding energy (eV) |
|---|---|---|
| N1$s$ | 4.00 N1$s$ | −409.90 |
| $\sigma_g 2s$ | 2.00 N2$s$ | −37.23 |
| $\sigma_u 2s$ | 2.00 N2$s$ | −18.60 |
| $\pi_u 2p$ | 4.00 N2$p$ | −16.80 |
| $\sigma_g 2p$ | 2.00 N2$p$ | −15.50 |

reducing the many-body problem to that of one active electron in some model potential [2]. Several first-order models have been developed using this theory. One of the most successful is the CDW-EIS model, where the initial and final state wave functions are given by

$$\chi_i^{+EIS} = \phi_i(\vec{x})\exp(-i\varepsilon_i t)\exp[-iv\ln(vs+\vec{v}\cdot\vec{s})] \quad (1)$$

and

$$\chi_f^{-CDW} = (2\pi)^{-3/2}\exp[i(\vec{k}\cdot\vec{x}-E_k t)] \times N^*(\xi)\,{}_1F_1(-i\xi;1;-ikx-i\vec{k}\cdot\vec{x}) \times N^*(\zeta)\,{}_1F_1(-i\zeta;1;-ips-i\vec{p}\cdot\vec{s}), \quad (2)$$

where $\vec{x}$ ($\vec{s}$) is the active electron position vector relative to the target (projectile), $\phi_i(\vec{x})$ is the active electron initial bound state, $\varepsilon_i$ is the corresponding orbital energy, and $\vec{v}$ is the collision velocity. In Eq. (2), $\vec{k}$ ($\vec{p}$) is the momentum of the ejected electron relative to the target (projectile) nucleus, $E_k = k^2/2$ the electron energy, $\nu = Z_P/v$, $\zeta = Z_P/p$, $\xi = Z_T^*/k$, and $Z_T^*$ is the effective charge of the target in the final state.

As can be observed from Eq. (1), the initial bound state of the active electron is affected by the presence of the Coulomb field of the projectile introduced through an eikonal phase. The final state [Eq. (2)] is proposed as a product of continuum states associated with the active-electron–residual-target and active-electron–projectile interactions (two-center approximation). To take into account the presence of passive electrons in multielectronic targets, the initial bound state is described by a Roothaan-Hartree-Fock (RHF) [7] or Slater-type [8] wave function. The interaction of the ejected electron with the residual target is simulated by an effective Coulomb field. The effective nuclear charge is chosen as $Z_T^* = \sqrt{-2n\varepsilon_i}$ where $n$ is the principal quantum number corresponding to each atomic subshell that constitutes the initial bound state of the active electron in the molecule.

The approximations to the initial and final target wave functions described above correspond in fact to a choice of different model potentials for the target in the two channels. As a consequence these bound and continuum states are not orthogonal. A proper way to do the calculation would be to choose the same model potential in both channels. However, it is well known that hydrogenic orbitals are not accurate enough to describe the outer electronic states, which give the most important contribution to the cross sections in the energy range that we consider here. On the other hand, there are no analytical wave functions for continuum states except the hydrogenic wave functions that we use here. A proper solution to this problem is to calculate numerically bound and continuum states from the same model potential. While this is possible, after a great deal of work, for atoms [9], there is no equivalent solution for molecules.

TABLE II. Population of the $N_2$ molecular orbitals.

| Molecular orbital | Population |
|---|---|
| N1$s$ | 4.00 N1$s$ |
| $\sigma_g 2s$ | 1.50 N2$s$ + 0.50 N2$p$ |
| $\sigma_u 2s$ | 1.47 N2$s$ + 0.53 N2$p$ |
| $\pi_u 2p$ | 4.00 N2$p$ |
| $\sigma_g 2p$ | 0.50 N2$s$ + 1.50 N2$p$ |

Another difficulty encountered in the case of molecules is related to their multicenter character. In the present work we will use a one-center approximation, to be described below, which, while not taking into account such details as the orientation and structure of the molecule, employs the correct binding energy.

### B. Ionization cross sections for molecular targets

A rigorous DDCS calculation for ionization of molecular targets would demand knowledge of the initial bound state and of the final continuum state of the ejected electron. Due to the complexity of the problem some type of approximation is necessary. In the present work we use two methods that allow us to obtain the ionization DDCS's for molecules through calculations carried out for atomic targets. The simplest one is Bragg's additivity rule. In this case, the DDCS is calculated as the sum of the DDCS corresponding to each atom of the molecule weighted by the number of atoms in the molecule. Thus, for the methane molecule ($CH_4$), the following calculation is carried out:

$$\sigma(CH_4) = \sigma(C) + 4\sigma(H), \quad (3)$$

where the atomic initial bound states of C are described by RHF wave functions.

The other way to calculate the DDCS is to take into account the molecular character of the target [4,5]. In this approximation, the ionization DDCS for each molecular orbital is calculated by making a lineal combination of atomic DDCS's, whose coefficients are obtained from a population analysis (which we will describe next). Finally, these partial

TABLE III. Population and binding energies of the $CH_4$ molecular orbitals.

| Molecular orbital | Population | Binding energy (eV) |
|---|---|---|
| C1$s$ | 2.000 C1$s$ | −290.70 |
| $2a_1$ | 1.133 C2$s$ + 0.867 H1$s$ | −22.90 |
| $1t_2$ | 3.399 C2$p$ + 2.601 H1$s$ | −12.60 |

TABLE IV. Population and binding energies of the CO molecular orbitals.

| Molecular orbital | Population | Binding energy (eV) |
|---|---|---|
| O1$s$ | 2.000 O1$s$ | −542.1 |
| C1$s$ | 2.000 C1$s$ | −295.9 |
| $1\sigma$ | 1.207 O2$s$+0.178 O2$p$+0.333 C2$s$+0.282 C2$p$ | −38.3 |
| $2\sigma$ | 0.627 O2$s$+0.985 O2$p$+0.386 C2$s$+0.002 C2$p$ | −20.1 |
| $1\pi$ | 2.980 O2$p$+1.020 C2$p$ | −17.2 |
| $3\sigma$ | 0.026 O2$s$+0.085 O2$p$+0.776 C2$s$+1.113 C2$p$ | −14.5 |

calculations are summed, taking into account the number of electrons in each molecular orbital.

#### *1. Molecular nitrogen* ($N_2$)

The electronic configuration of the ground state is $(N1s)^4(\sigma_g 2s)^2(\sigma_u 2s)^2(\pi_u 2p)^4(\sigma_g 2p)^2$. In Table I the populations and binding energies corresponding to each molecular orbital are presented. These values have been obtained from an analysis of the intensities of the spectral lines corresponding to the different orbitals [10]. Comparing the spectrum of $N_2$ with that of Ne (in which it is observed that the $2s$ subshell gives a line about nine times larger per electron than the $2p$ subshell), it is deduced qualitatively that the orbital $\sigma_u(2s)$ would have more $2s$ character than $\sigma_g(2s)$, which in turn presents a larger $2s$ character than $\sigma_g(2p)$. On the other hand, for symmetry reasons, the orbital $\pi_u(2p)$ presents only $2p$ character. Keeping this in mind and respecting the total number of electrons $2s$ and $2p$ contributed by the nitrogen atoms we have obtained the values showed in this table. Another method to calculate the populations is that of molecular orbitals constructed from a lineal combination of atomic orbitals in a self-consistent field (MO-LCAO-SCF) [11]. In Table II we show the populations estimated with this method. Calculations carried out with these last values (using the orbital energies given in Table I) show that the DDCS's do not vary in a significant way in comparison with those calculated using the values given in Table I, since the observed differences were smaller than 1%. Therefore, for reasons of simplicity, in all the calculations we will use the values given in Table I.

#### *2. Methane* ($CH_4$)

Methane presents the following electronic configuration in the ground state: $(C1s)^2(2a_1)^2(1t_2)^6$. In Table III the binding energies and atomic populations calculated with the MO-LCAO-SCF method for each molecular orbital are given [12]. With these values, the molecular DDCS is calculated as follows:

$$\sigma(CH_4)=\sigma(C1s)+\sigma(2a_1)+\sigma(1t_2) \tag{4}$$

where

$$\sigma(C1s)=2.000\sigma(C1s), \tag{5}$$

$$\sigma(2a_1)=1.133\sigma(C2s)+0.867\sigma(H1s), \tag{6}$$

$$\sigma(1t_2)=3.399\sigma(C2p)+2.601\sigma(H1s). \tag{7}$$

#### *3. Carbon monoxide (*CO*)*

Carbon monoxide, in its ground state, has four core electrons [O(1$s$),C(1$s$)] and another ten electrons distributed in four molecular orbitals as $(1\sigma)^2(2\sigma)^2(1\pi)^4(3\sigma)^2$. A detailed analysis of this molecule has been carried out in [13]. It was observed that, whereas the individual molecular orbitals are all strongly polar, the molecule as a whole is almost nonpolar (calculations of gross charge on each atom give very small values). Another remarkable characteristic is that the CO molecule achieves almost as strong $\pi$ and $\sigma$ bonding as in the isoelectronic molecule $N_2$. This would explain the close similarity in the physical properties of the two molecules. The electronic populations have been calculated using the MO-LCAO-SCF method. In Table IV these values are shown together with the experimental binding energies [10].

#### *4. Carbon dioxide* ($CO_2$)

The data corresponding to $CO_2$ are presented in Table V. These values were obtained in [14]. The binding energies have been extracted from the experimental spectra while the population analysis has been carried out using the complete neglect of differential overlap (CNDO) method [10].

## III. RESULTS AND DISCUSSIONS

### A. Doubly differential cross sections

In order to test the different models we have chosen some particular cases of proton impact on $CO_2$ and $CH_4$ at intermediate to high energies. In Fig. 1 the theoretical and experimental DDCS's for single ionization of $CO_2$ by impact of

TABLE V. Population and binding energies of the $CO_2$ molecular orbitals.

| Molecular orbital | Population | Binding energy (eV) |
|---|---|---|
| O1$s$ | 4.000 O1$s$ | −540.8 |
| C1$s$ | 2.000 C1$s$ | −297.5 |
| $3\sigma_g$ | 1.278 O2$s$+0.164 O2$p$+0.558 C2$s$ | −39.7 |
| $2\sigma_u$ | 1.306 O2$s$+0.130 O2$p$+0.564 C2$s$ | −37.5 |
| $4\sigma_g$ | 0.594 O2$s$+1.026 O2$p$+0.380 C2$s$ | −19.4 |
| $3\sigma_u$ | 0.544 O2$s$+1.120 O2$p$+0.336 C2$p$ | −18.1 |
| $1\pi_u$ | 2.492 O2$p$+1.508 C2$p$ | −17.6 |
| $1\pi_g$ | 4.000 O2$p$ | −13.8 |

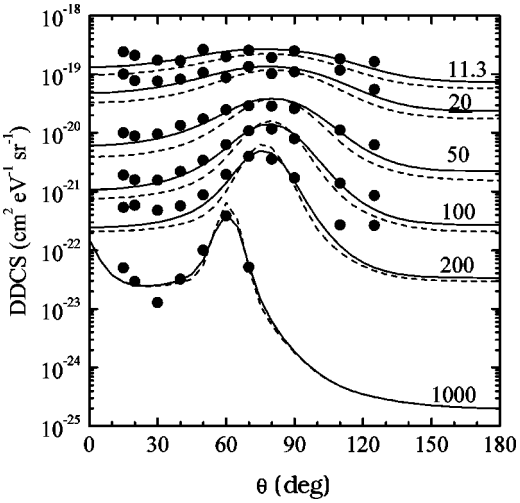


FIG. 3. Same as Fig. 1, but for 2 MeV proton impact on $CH_4$.

FIG. 1. DDCS for single ionization of $CO_2$ by 300 keV proton impact as a function of electron emission angle for fixed values of electron energy, in eV. Theory: solid line, CDW-EIS-MO; dashed line, CDW-EIS; dash-dotted line, CDW-EIS-MO but using RHF instead of Slater-type functions. Experiments: (●), from [5].

300 keV protons are shown as a function of the electron emission angle at fixed final electron energies. Here we employ three different approximations.

(1) Bragg's additivity rule, which will be labeled CDW-EIS. In order to have a good representation of the initial atomic bound states we employ RHF wave functions, which are, as is well known, better than the use of Slater-type orbitals.

(2) A molecular description of the target initial state, which we call hereafter CDW-EIS-MO, where the atomic orbitals used to construct the molecular orbitals are represented by Slater-type functions.

(3) A molecular description of the target initial state where the atomic orbitals used to construct the molecular orbitals are represented by RHF wave functions.

As can be observed, between the two molecular descriptions CDW-EIS-MO gives the better agreement between experiments and theory. This behavior could be expected from the fact that the electronic populations have been obtained using Slater-type orbitals. Calculations with Bragg's rule underestimate the experiments at small emission angles.

It must be noted that variations in the molecular orbital binding energies can produce changes in the theoretical results. The best agreement is obtained using the experimental values instead of those calculated through the MO-LCAO-SCF or CNDO methods. Therefore we have decided to use these values in all the calculations. In Figs. 2 and 3, theoretical calculations performed with CDW-EIS and CDW-EIS-MO and experimental DDCS's for single ionization of $CH_4$ by impact of 250 keV and 2 MeV protons, respectively, are shown. As we can observe in the figures the molecular method gives better results and, at the lower electron energies considered, the calculations are in good agreement with the experiments for electron angles smaller than 100°. At

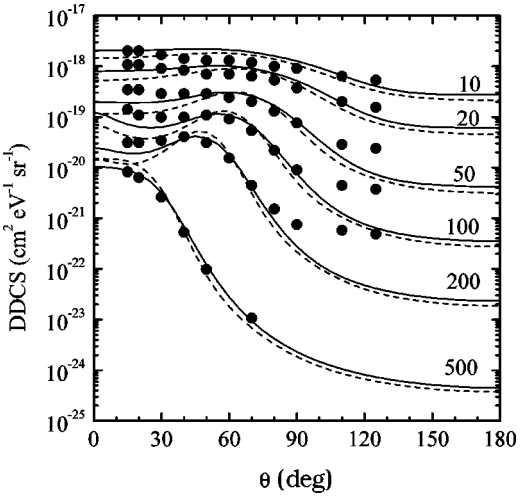


FIG. 2. Same as Fig. 1, but for 250 keV proton impact on $CH_4$.

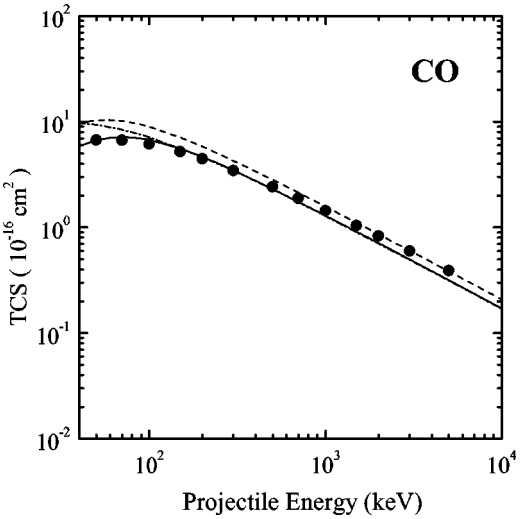


FIG. 4. TCS for single ionization of CO by proton impact as a function of projectile energy. Theory: solid line, CDW-EIS-MO; dashed line, CDW-EIS; dash-dotted line, B1-MO. Experiments: (●), from [6].

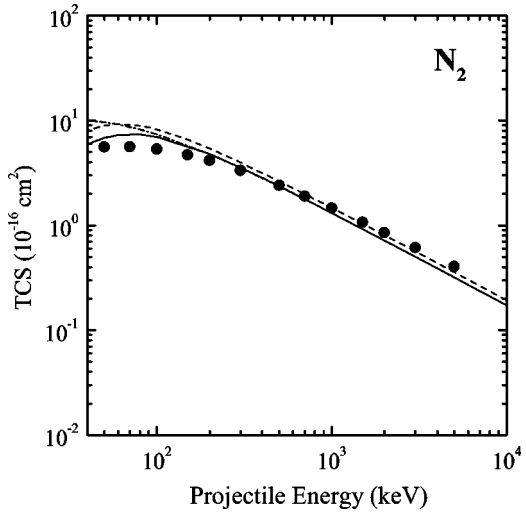


FIG. 5. Same as Fig. 4, but for proton impact on $N_2$.

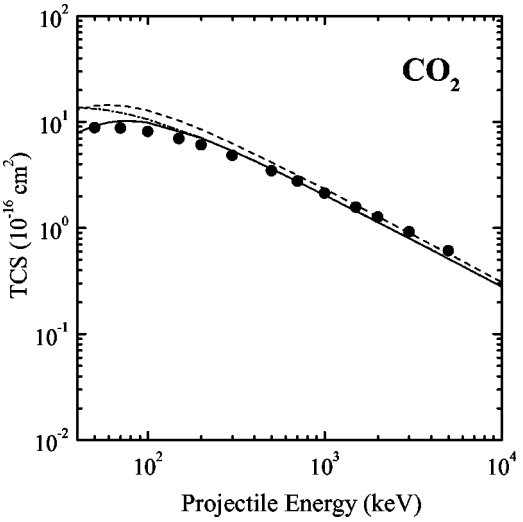


FIG. 6. Same as Fig. 4, but for proton impact on $CO_2$.

larger angles, the theoretical calculations underestimate the experimental data. This behavior has been observed previously for atomic targets and it has been shown that it can be corrected by using more accurate wave functions for the initial bound and final continuum states of the target [9]. In such a case these states must be calculated numerically, solving the time-independent Schrödinger equation with a model potential. This method, which is much more complex than using analytical approximations like the present ones, is clearly beyond our present capabilities and it has still not been solved. However, the agreement is quite good in almost all the angular range, proving the usefulness of the CDW-EIS-MO model.

### B. Total cross sections

In Figs. 4, 5, and 6 we present theoretical results from CDW-EIS and CDW-EIS-MO calculations in comparison with experimental total cross sections for single ionization of CO, $N_2$, and $CO_2$ by proton impact. From these graphs we can see that the calculations carried out with the molecular method are in very good agreement with the experimental data at intermediate and high energies. While both theoretical methods give similar results at high energies, there are differences in the region of the maximum corresponding to the intermediate energy range where CDW-EIS overestimates the experimental data. This shows that Bragg's rule should be used with caution and that its validity range is restricted to high impact energies. Also presented in the figures are results from a first Born calculation (B1-MO) using the same molecular model used in the CDW-EIS-MO calculation. Both models present the same asymptotic behavior as the energy increases, as one would expect since the effect of the distortion diminishes. On the other hand, large differences appear, for all targets, at energies below 200 keV where B1-MO largely overestimates the experimental data. It is clear that a B1 calculation using Bragg's additivity rule would give even worse results. This is clear evidence that application of this rule at intermediate energy must be done with extreme caution [15] and higher-order calculations, like CDW-EIS-MO, should be preferred. Finally, we can also observe that the CO and $N_2$ molecules present very similar values of TCS's, in agreement with the analysis carried out in the preceding section.

## IV. CONCLUSIONS

We have made an extension of the CDW-EIS model which allows us to calculate doubly differential and total cross sections for single ionization of molecular targets. Two approaches were used to carry out these calculations: one that takes into account the molecular character of the target and Bragg's additivity rule. Applying the former we obtain better results, thus proving the limited range of validity of Bragg's additivity rule in the region of high impact energy. Comparison with first Born calculations using the molecular model shows that higher-order models, like CDW-EIS, are required to get good agreement with experiments at intermediate impact energy.

## ACKNOWLEDGMENTS

This research was supported in part by the Agencia Nacional de Promoción Científica y Tecnológica (Argentina) under Contract No. PICT98 03-04262 and by the Cooperation Program SCyT (Argentina)–ECOS (France), Grant No. A98E02. M.E.G. and R.D.R. also acknowledge the Consejo Nacional de Investigaciones Científicas y Técnicas (Argentina).

[1] G.H. Olivera, A.E. Martínez, R.D. Rivarola, and P.D. Fainstein, Radiat. Res. **144**, 241 (1995); Nucl. Instrum. Methods Phys. Res. B **111**, 7 (1996).

[2] P.D. Fainstein, V.H. Ponce, and R.D. Rivarola, J. Phys. B **21**, 287 (1988).

[3] P.D. Fainstein, V.H. Ponce, and R.D. Rivarola, J. Phys. B **24**, 3091 (1991).

[4] B. Senger and R.V. Rechenmann, Nucl. Instrum. Methods

Phys. Res. B **2**, 204 (1984).
[5] B. Senger, Z. Phys. D: At., Mol. Clusters **9**, 79 (1988).
[6] M.E. Rudd, Y.-K. Kim, D.H. Madison, and J.W. Gallagher, Rev. Mod. Phys. **57**, 965 (1985).
[7] E. Clementi and C. Roetti, At. Data Nucl. Data Tables **14**, 177 (1974).
[8] J.C. Slater, Phys. Rev. **36**, 57 (1930).
[9] L. Gulyás, P.D. Fainstein, and A. Salin, J. Phys. B **28**, 245 (1995).
[10] K. Siegbahn, C. Nordling, G. Johansson, H. Hedman, P. F. Hedén, K. Hamrin, U. Gelius, T. Bergmark, L. O. Werme, R. Manne, and Y. Baer, *ESCA Applied to Free Molecules* (North-Holland, Amsterdam, 1969).
[11] C.W. Scherr, J. Chem. Phys. **23**, 569 (1955).
[12] R. Hoffmann, J. Chem. Phys. **39**, 1397 (1963).
[13] R.S. Mulliken, J. Chem. Phys. **23**, 1833 (1955).
[14] C.J. Allan, U. Gelius, D.A. Allison, G. Johansson, H. Siegbahn, and K. Siegbahn, J. Electron Spectrosc. Relat. Phenom. **1**, 131 (1972/73).
[15] D.I. Thwaites, Nucl. Instrum. Methods Phys. Res. B **69**, 53 (1992).